HHS Public Access

Author manuscript

Leukemia. Author manuscript; available in PMC 2020 August 14.

Published in final edited form as:

Leukemia. 2020 August ; 34(8): 2150–2162. doi:10.1038/s41375-020-0745-9.

A novel BCMA PBD-ADC with ATM/ATR/WEE1 inhibitors or bortezomib induce synergistic lethality in multiple myeloma

Lijie Xing[1,2], **Liang Lin**[1], **Tengteng Yu**[1], **Yuyin Li**[1], **Shih-Feng Cho**[1,3,4], **Jiye Liu**[1], **Kenneth Wen**[1], **Phillip A Hsieh**[1], **Krista Kinneer**[5], **Nikhil Munshi**[1], **Kenneth C Anderson**[1], **Yu-Tzu Tai**[1]

[1]Jerome Lipper Multiple Myeloma Center, LeBow Institute for Myeloma Therapeutics, Dana-Farber Cancer Institute, Harvard Medical School, Boston MA, USA

[2]Department of Hematology, Shandong Provincial Hospital affiliated to Shandong University, Jinan, Shandong, 250021, People's Republic of China

[3]Division of Hematology & Oncology, Department of Internal Medicine, Kaohsiung Medical University Hospital, Kaohsiung Medical University, Kaohsiung, Taiwan

[4]Faculty of Medicine, College of Medicine, Kaohsiung Medical University, Taiwan

[5]Oncology Discovery, AstraZeneca, Gaithersburg, MD, USA

Abstract

To target mechanisms critical for multiple myeloma (MM) plasma cell adaptations to genomic instabilities and further sustain MM cell killing, we here specifically trigger DNA damage response (DDR) in MM cells by a novel BCMA antibody drug conjugate (ADC) delivering the DNA cross-linking PBD dimer tesirine, MEDI2228. MEDI2228, more effectively than its anti-tubulin MMAF-ADC homolog, induces cytotoxicity against MM cells regardless of drug resistance, BCMA levels, p53 status, and the protection conferred by bone marrow stromal cells and IL-6. Distinctly, prior to apoptosis, MEDI2228 activates DDRs in MM cells via phosphorylation of ATM/ATR kinases, CHK1/2, CDK1/2, and H2AX, associated with expression

*To whom correspondence should be addressed: Yu-Tzu Tai, Ph.D., Department of Medical Oncology, Dana-Farber Cancer Institute, M551, 450 Brookline Avenue, Boston, MA 02215. Phone: (617) 632-3875; Fax: (617) 632-2140; yu-tzu_tai@dfci.harvard.edu; Kenneth C Anderson, M.D., Department of Medical Oncology, Dana-Farber Cancer Institute, M557, 450 Brookline Avenue, Boston, MA 02215 Phone: (617) 632-2144; Fax: (617) 632-2140; Kenneth_anderson@dfci.harvard.edu.

Authorship Contributions

Conception and design: Y-T Tai, K Kinneer, K C Anderson

Development of methodology: L Xing, L Lin, T Yu, Y Li, J Liu, S-F Cho

Acquisition of data (provided reagents, facilities, etc.): L Xing, L Lin, T Yu, Y Li, J Liu, S-F Cho, K Wen, P A Hsieh

Reagents and Materials: K Kinneer

Analysis and interpretation of data (statistical analysis, biostatistics analysis): L Xing, L Lin, T Yu, Y Li, S-F Cho, J Liu, K Wen, P A Hsieh, Y-T Tai

Provided and managed patients: N Munshi, KC Anderson

Writing, review, and/or revision of the manuscript: L Xing, K Kinneer, Y-T Tai, KC Anderson

Study supervision: K C Anderson, Y-T Tai

Conflicts of Interest Disclosures

K Kinneer is an employee of AstraZeneca and has stock and/or stock interests in AstraZeneca. N.C.M. serves on advisory boards to Millennium-Takeda, Celgene, and Novartis. K.C.A. serves on advisory boards Celgene, Millennium-Takeda, Bristol-Myers Squibb, Gilead Sciences, Janssen, and Sanofi-Aventis and is a Scientific founder of OncoPep and C4 Therapeutics. All other authors declare no competing financial interests.

of DDR-related genes. Significantly, MEDI2228 synergizes with DDR inhibitors (DDRi s) targeting ATM/ATR/WEE1 checkpoints to induce MM cell lethality. Moreover, suboptimal doses of MEDI2228 and bortezomib (btz) synergistically trigger apoptosis of even drug-resistant MM cells partly via modulation of RAD51 and accumulation of impaired DNA. Such combination further induces superior in vivo efficacy than monotherapy via increased nuclear γH2AX-expressing foci, irreversible DNA damages and tumor cell death, leading to significantly prolonged host survival. These results indicate leveraging MEDI2228 with DDRi s or btz as novel combination strategies, further supporting ongoing clinical development of MEDI2228 in patients with relapsed and refractory MM.

Keywords

multiple myeloma, MM; B cell maturation antigen, BCMA; antibody drug conjugate, ADC; pyrrolobenzodiazepine, PBD; monomethyl auristatin F, MMAF; bortezomib, btz; lenalidomide, len; pomalidomide, pom; bone marrow stromal cells, BMSCs; interleukin-6, IL-6; DNA damage response, DDR; double strand break, DSB; DDR inhibitor, DDRi; DNA repair; Ataxia-Telangiesctasia mutated, ATM; ATR, ataxia telangiectasia and Rad3-related protein; WEE1; drug resistance; synthetic cytotoxicity

Introduction

Multiple myeloma (MM) is a malignancy of clonal plasma cells with ongoing DNA damages associated with progression from pre-malignant monoclonal gammopathy of undetermined significance (MGUS) to active MM [1–4]. Hallmarks of MM include accumulated DNA lesion-induced genomic aberrations and genomic instabilities, resulting in clonal evolution and treatment resistance [5–8]. Current therapies combining conventional corticosteroids and alkylating agents with proteasome inhibitors (PIs), immunomodulatory drugs (IMiDs), and monoclonal antibodies (mAbs) have markedly increased overall survival [9–11]. Nonetheless, the development of drug resistance underlies relapse of disease, and there remains an unmet need for novel treatments targeting new mechanisms of action, as well as novel immunotherapeutic approaches.

The first two mAbs elotuzumab and daratumumab, targeting SLAMF7 [12] and CD38 [13], respectively, were FDA approved for treatment of relapsed and refractory MM (RRMM) in 2015 in combination with lenalidomide (len) and dexamethasone (dex) [14–16]. More recent clinical trials of these two mAbs have shown activity in newly diagnosed and smoldering MM (SMM) [17–20]. New therapeutic mAbs are being developed to target other MM antigens and/or enhance effector cell-mediated tumor cell lysis. In addition, antibody-drug conjugates (ADCs) generated by linking mAbs to potent cytotoxic chemoreagents have also shown clinical benefits [21]. Specifically, the first MM ADC GSK2857916 [22] was developed to target B cell maturation antigen (BCMA), a more selective MM antigen than either SLAMF7 or CD38, and conjugated to a microtubule disrupting monomethyl auristatin-F (MMAF) [22–26]. This ADC selectively induces significant in vitro and in vivo anti-MM activities in preclinical studies [22, 27], and further induces responses in heavily pretreated RRMM resistant to dex, bortezomib (btz), IMiDs, and daratumumab [28, 29]. Meanwhile, remarkable responses have been observed in clinical trials of BCMA-directed

chimeric antigen receptor (CAR)-modified T cells [30–32] and bispecific T cell engagers [33, 34]. All these studies have validated BCMA as an excellent target MM antigen for novel immunotherapies.

Most recently, a new BCMA-targeting ADC MEDI2228 was developed to preferentially bind to membrane-bound vs soluble BCMA, and thereby more efficiently deliver the pyrrolobenzodiazepine (PBD) payload tesirine to MM cells [35]. PBD dimers, a class of DNA minor groove interstrand crosslinking (ICL) agents, may provide advantages in targeting low expressing antigens and the dormant minute tumor-initiating cell populations, even at low drug-antibody ratios (DARs) of ADCs. MEDI2228 targets MM cells, including CD19+CD138− MM progenitor cells in an in vitro preclinical study [35]. Similar PBD-based ADCs targeting different cancer antigens are currently being clinically evaluated in cancers including small lung cancer [36] and B-cell tumors [37]. Here we investigate the effectiveness and molecular mechanisms of MEDI2228 vs its MMAF-ADC homolog to overcome drug resistance and target MM cells expressing low levels of BCMA and with p53 mutations in the bone marrow (BM) microenvironment. We further explore synthetic lethal strategies of combining MEDI2228 with DNA damage repair (DDR) inhibitors or btz in MM. Our results support current clinical development of MEDI2228 and provide the framework to treat RRMM with this BCMA-targeting PBD-ADC, alone or together with DDRi s or btz, to prolong survival especially in RRMM.

Materials and Methods

Generation of anti-BCMA ADCs

MEDI2228 (herein referred to as M2) was prepared through site-specific conjugation of the PBD dimer, tesirine, to the BCMA-Ab1 antibody using a protease-cleavable linker, as previously described [35]. The ADC M3 was similarly generated by attaching monomethyl auristatin F (MMAF) payload to the antibody BCMA-Ab1. Both payloads were site-specifically conjugated to an engineered cysteine at the 239i position in the BCMA-Ab1, resulting in an ADC with a drug-to-antibody ratio (DAR) of 2 [38]. Briefly, the BCMA-Ab1 was reduced with 40 molar excess of TCEP for three hours at 37°C, followed by three successive dialyses to remove the TCEP. The antibody was then oxidized with 20 molar excess of DHAA for four hours at room temperature, and then conjugated using eight molar equivalence of payload. After conjugation, the free payload and protein aggregate were removed by Ceramic Hydroxyapatite purification.

Analysis of tumors harvested from mice using immunoblotting and immunostaining

Following 3d-treatment, tumor from each group was harvested, and cell lysates were made for immunoblotting. Sections of tumors collected from mice were subjected to immunohistochemical staining for proliferation by Ki67(CRM325, Biocare Medical) and DNA damage by γH2AX (CST-9718, Cell Signaling Technology), with counterstaining by DAPI (CST-4083, Cell Signaling Technology) to locate nuclei. Immunohistochemical images were taken on Zeiss Inverted Fluorescence Microscope for Ki67. The confocal images for γH2AX were acquired using a Zeiss LSM 880 confocal microscope and Zen

Black image acquisition software [39, 40]. A Plan-Apochromat 63X/1.40 Oil DIC M27 objective lens was used.

Results

MEDI2228 (M2) induces more potent cytotoxicity than its MMAF-ADC homolog (M3) in MM cell lines regardless of p53 status and drug resistance

We first evaluated cytotoxicity of a novel BCMA PBD-ADC MEDI2228 (M2) vs its MMAF-ADC homolog (M3) against a panel of MM cell lines. Both ADCs are composed of the same anti-BCMA mAb but are conjugated to different payloads: a DNA cross-linking PBD tesirine for M2 and a microtubule binding MMAF for M3. Using the 3d CCK8-based viability assay, ED_{50} values are lower than those of M3 in all tested MM cell lines (n=10) expressing various BCMA levels, regardless of sensitivity to current anti-MM therapies including dex and IMiDs (lenalidomide (len) and pomalidomide (pom)) [39, 41] (Fig. 1a, Supplemental Fig. S1A–C). In these MM cell lines (n=8), not including RPMI8226 (RPMI) and its derived BCMA-overexpressing RPMI-BCMA [42], ED_{50} values derived from the 3d CCK8 assay, range from 11.85 to 3499 ng/ml and 21.28 to 271431 ng/ml for M2 and M3, respectively. All MM cells harbor various p53 mutations, except MM1S and H929 cells from which two IMiDs-resistant MM1S(R) and H929(R) cells are derived, respectively. M2, but not M3, significantly induces cytotoxicity against RPMI8226 cells expressing the lowest BCMA levels and relative resistance to IMiDs (Fig. 1a–b, Supplemental Fig. S1A). Using DNA synthesis assay, M2 even shows greater (>1–2-log) potency than M3 in blocking proliferation of all MM cells (left panel in Fig. 1b, Supplemental Fig. S1D). For example, ED_{50} values for M2 vs M3 are 189.7 vs 21427 ng/ml in RPMI8226 cells, indicating >2-log higher potency of M2 vs M3 in this MM cell line with lowest BCMA. M2, but not M3, significantly decreased viability of both ANBL6 and its derivative bortezomib (btz)-resistant ANBL6-BR cells (Supplemental Fig. S1E) cultured with IL-6 (Fig. 1b right panel). These paired IL-6-dependent ANBL6 cells are relatively insensitive to M3, as RPMI8226 cells. These data indicate that MM cells with relatively lower BCMA expression are also significantly more susceptible to M2 vs M3. Using flow cytometry (FCM) analysis following staining with Annexin V and live/dead Aqua, M2 induces earlier and significantly increased apoptosis in paired MM cell lines sensitive or resistant to dex or btz in a dose- and time-dependent manner, when compared with M3 (Fig. 1c, Supplemental Fig. S1F).

These results indicate that M2 overcomes resistance to current anti-MM drugs (dex, len, pom, btz) to a greater extent than M3 in MM cells, regardless of BCMA levels and drug resistance.

M2 is more effective than M3 in inducing cytotoxicity against MM cell lines and patient MM cells protected by the bone marrow microenvironment

We next assessed cytotoxicity of M2 and M3 in MM cells co-cultured with bone marrow stromal cells (BMSCs) and IL-6, two key BM components to confer MM cell growth, survival, and drug resistance. Using BLI- (Fig. 2a) and FCM-based (Supplemental Fig. S2A) assays, M2, more potently than M3, inhibits viability of MM1Sluc (Fig. 2a) and IMiD-resistant MM cells including H929(R) and MM1S(R) (Supplemental Fig. S2A). M2 still

effectively blocks btz-resistant ANBLR-BR cells (Fig. 2b) and other tested MM cell lines (Supplemental Fig. S2B) co-cultured with BMSCs, with minimal impact on BCMA-negative BMSCs, PBMCs, and NK cells (Fig. 2b, Supplemental Fig. S2C). In addition, M2 blocks growth and survival of H929 MM cells stimulated by IL-6 (Supplemental Fig. S2D).

Importantly, in freshly isolated CD138+ patient MM cells, M2-induced apoptotic fraction is >2-fold when compared with M3 (Fig. 2c). Further, BM mononuclear cells from patients were incubated with M2 to test effects of M2 on patient MM cells protected by their BM supporting cells. M2 significantly depletes viable CD138+CD38high BM cells from patients with newly diagnosed MM (NDMM) (n=2) and RRMM (n=12) (Fig. 2d, Supplemental Fig. S2E). Thus, M2 is more cytotoxic to MM cells in the BM microenvironment than M3 and depletes patient MM cells regardless of disease status and protection by BM supporting cells.

M2 significantly activates DNA damage response and repair signaling cascades, followed by apoptosis, in drug-sensitive and -resistant MM cells

Using immunoblotting, we next determine induction of DNA damage response (DDR) signaling cascades triggered by M2 in MM cell lines. in a time- and dose-dependent manner, M2, but not M3, induces phosphorylation of ATM, cell cycle checkpoint kinase 1 (CHK1), and CHK2 (CHK1/2), as well as histone 2AX (H2AX), an early event in the DNA double strand break (DSB) response (Fig. 3a, Supplemental Fig. S3A). M2-stimulated phosphorylation of ATM and CHK1/2 is detected at 4h and sustained for >1d following treatment. Earlier and more pronounced activation of ATM and CHK1/2 triggered by M2 was seen in H929 cells which express significantly higher BCMA levels than MM1S cells (Fig. 1a–b, Supplemental Fig. S3A, C). The intensity of M2-induced phosphorylation of ATM and CHK1/2 also correlated with BCMA levels derived from the parental RPMI8226 MM cells (Supplemental Fig. S3D). Of note, M2-induced phosphorylation of ATM and CHK1/2 occurs to a significantly greater extent than phosphorylation of ATR, in MM cells tested. Following 2d-treatment with M2, cleavage of PARP (cPARP) and caspase 3 (cCas3) is induced in a BCMA-dependent manner (Supplemental Fig. S3B, E–F), associated with increased phosphorylated H2AX (γH2AX) (Supplemental Fig. S3B), indicating that M2 induces DNA damages followed by apoptosis in MM cells. Importantly, M2 dose-dependently induces phosphorylation of ATM and CHK1/2 in all MM cells, including 6 cell lines with p53 mutations (Fig. 3b–c). Under the same treatment conditions as M2, M3 induce neither ATM/ATR nor CHK1/2 (Supplemental Fig. S3A). M2 is more effective than M3 in inducing cPARP and cCas3 (Supplemental Fig. S3F), consistent with its higher potency than M3 in triggering MM cell apoptosis (Fig. 1–2). Significantly, M2 triggered ATM/ATR and downstream CHK1/2 signaling pathways, γH2AX and PARP cleavage in ANBL6 and the paired btz-resistant ANBL6-BR cells (Fig. 3c). Prominent activation of ATM and CHK1/2 by M2 is also seen in IMiD-resistant H929(R) cells to a similar extent as the parental H929 MM cells (Fig. 3d). Thus, in btz- and len-resistant MM cells, M2 still induces BCMA-dependent DDR signaling pathways via activation of ATR/ATM-CHK1/2 signaling cascade, followed by apoptosis.

Analysis of DNA repair mechanism TaqMan® array next show that M2 changes expression of DNA damage repair-associated genes (51 out of 72) in H929 MM cells (Fig. 4a). In various drug-sensitive and -resistant MM cells (n>6), M2, in a dose-dependent fashion, induces RAD51, which binds to DNA ICLs before a DSB is generated [43] (Fig. 4b–c), whereas M3 does not (Supplemental Fig. S3G). Thus, in MM cells, M2 specifically activates ATM/ATR-CHK1/2-mediated DDR signaling cascades and induces downstream DDR-related molecules associated with increased γH2AX and RAD51, followed by apoptosis.

DDR inhibitors targeting ATM/ATR/WEE1 potentiate M2-induced MM cell cytotoxicity

Since M2 significantly induces ATM/ATR-CHK1/2 DDR signaling cascades before apoptosis in all MM cells tested, we next asked whether DDR inhibitors (DDRi s) targeting these molecules further enhance sensitivity of MM cells to M2. These essential regulators of responses to DNA damage, including DSB and replication stress, have stimulated both pre-clinical and clinical development of highly selective small molecules [44] including AZD0156 [45], AZD6738 [46], and AZD1775 [47] targeting ATM, ATR, and WEE1, respectively. All these DDRi s show dose-dependent cytotoxicity against MM cells as single agent, due to constitutively ongoing DNA damage in the majority of MM cells [1–3]. Importantly, these DDRi s combined with M2 at low doses (< ED_{50}) augment cytotoxicity even against IMiDs-resistant MM1S(R) than either drug alone (Fig. 5a). Low doses of these DDRi s significantly improve responses to M2 in other MM cell lines (n>5) (Supplemental Fig. S4A–B). Results from CTG-based viability assays were analyzed to calculate combination indices (CIs) [42, 48]. CI values of less than 1 further indicate synergistic cytotoxicity induced by combined M2 with DDRi s in all tested MM cell lines (n>5). In contrast, AZD6738 did not enhance M3-induced cytotoxicity in RPMI8226 MM cells (Supplemental Fig. S4C, lower panel). Immunoblotting analysis confirms that ATMi (AZD0156) specifically blocks phosphorylated ATM and downstream CHK1/2 signaling induced by M2 in all MM cells tested (Fig. 5b, Supplemental Fig. S4D). Similar results were seen when an additional ATMi (KU55933) was used (Supplemental Fig. S4E). M2 also induces G2/M checkpoint WEE1-associated phosphorylation of CDK1/2 (n=6, Supplemental Fig. S4F). Conversely, disruption of the G2/M checkpoint by WEE1i AZD1775 blocks M2-induced pCDK1/CDK2 in MM1S(R) cells (Fig. 5c). Such combination treatment accelerates MM cells with deregulated G1 checkpoints to premature mitotic entry, resulting in further catastrophe and apoptosis.

M2, combined with bortezomib, induces synergistic cytotoxicity against MM cells in vitro and in vivo

Since btz is standard of care in current MM treatment and btz inhibits certain DNA-damage repair pathways, i.e., RAD51 [49], we next evaluate whether the addition of btz alters RAD51 induced by M2. Using immunoblotting and immunofluorescence followed by confocal microscopy analysis, M2 induces RAD51, which is downregulated by btz (Fig. 6a–b). As shown in JJN3 and RPMI8226 cells, M2-induced RAD51 is reduced by combined btz and M2 treatments. Numbers of M2-increased RAD51 foci (green) were significantly decreased by the co-treatments with M2 and btz, associated with significant accumulation of γH2AX foci (red) in representative JJN3 and RPMI8226 MM cells which are relatively less sensitive to M2 (Fig. 6b). M2, together with btz significantly augmented degrees of DNA

damages caused by either agent alone. Accumulated DNA damage, accompanied by attenuated homologous recombination (HR) repair activity, led to significantly increased MM cell death, as shown in Annexin V/PI-based FMC analysis (Fig. 6c, Supplemental Fig. S5A). Combined M2 and btz at low doses of each drug for 2d further enhances apoptosis in JJN3 and RPMI8226 cells, when compared with either agent alone ($p<0.01$). Significantly increased cell death following combined treatments is also seen in btz-resistant ANBL6-BR cells cultured with IL-6. CIs < 1 are further obtained in 3 representative MM cells relatively resistant (Fig. 6d, Supplemental Fig. S5B) and sensitive (Supplemental Fig. S5C) to M2. These results indicate synergistic cytotoxicity of M2 plus btz.

In vivo efficacy of sub-optimal doses of M2 with btz was next evaluated in the MM1S xenograft mouse model. An M2 dose of 0.4 mg/kg was sub-optimal, since it results in tumor growth inhibition but not a durable regression in this model. This dose of M2 allowed for the detection of combination effects if they exist. Mice with palpable MM1S tumors were randomized into 4 groups receiving either vehicle control, a single treatment of M2, or 6 treatments of btz (0.4mg/kg for each treatment) alone or with M2. At 24d after treatment, a single dose of M2 or a total of 6 doses of btz significantly delays MM1S tumor growth in mice, compared with vehicle control (Fig. 7a, $p<0.005$, Supplemental Fig. S6A). Combination treatment significantly decreased tumor volume vs either agent alone ($p<0.04$) and did not result in body weight loss (Supplemental Fig. S6B). Follow-up for 177d shows a significant prolongation in median overall survival in the combination treated-group vs cohorts treated with either agent alone (cnt, 22d; M2, 40.5d; btz, 35d; M2+btz, 57d) ($p< 0.04$) (Fig. 7b). At 177d, 15% mice are still alive without any tumor growth in the combination-treated group.

Immunoblotting analysis of MM1S tumors harvested from mice after 3d treatment with M2 was done to determine whether M2 activates DDR signaling pathway in MM1S cells grown in vivo (Fig. 7c). In MM1S xenografted tumors, M2 significantly activates ATM-CHK1/2 pathway and upregulates γH2AX and RAD51, associated with increased growth arrest molecule p21 and apoptosis molecules (cPARP and cCas3). Immunohistochemistry for Ki67 further confirms more potent inhibition of proliferation after combined vs single-agent treatment (Fig. 7d, upper panel). Furthermore, immunofluorescence staining followed by confocal imaging demonstrates significantly enhanced γH2AX-positive micronuclei formation triggered by M2 vs btz (Fig. 7d, lower panel). Importantly, γH2AX-containing nuclear micro-foci are further augmented by treatment with combination vs either drug alone (Fig. 7d, right, $p<0.02$, Supplemental Fig. S6C), indicating enhanced DNA damage accumulation following combined vs single-agent treatments. Thus, the synergistic cytotoxicity of M2 with btz observed in vitro at the cellular level is translated into superior in vivo efficacy in the plasmacytoma model of MM.

Discussion

Here we show that selective targeting of critical DDR pathways exploited by MM plasma cells to adapt and survive to genotoxic stresses by a novel BCMA PBD-ADC represents a novel immunotherapeutic approach to overcome drug resistance in MM. Since disease relapse remains a major obstacle to prolong survival in MM, novel therapies with distinct

mechanisms of action are urgently needed to address the unmet medical need in RRMM. We evaluate the potency of the BCMA PBD-ADC MEDI2228 in preclinical models of MM drug resistance, and further investigate this ADC in combination with inhibitors of core components of DNA repair system or btz. The same drug: antibody ratio (DAR) 2 MMAF-ADC homolog was included in order to understand the contribution of the PBD warhead to the observed activity as mono- and combination therapy.

MEDI2228 has superior cytotoxicity against all MM cell lines and patient MM cells tested than its MMAF-ADC homolog, due to its distinct mechanisms of action. MEDI2228, but not its MMAF-ADC homolog, induces multiple DDR and cell cycle checkpoint signaling cascades including phosphorylation of ATM, CHK1/2, and CDK1/2 in MM cells. The potent cytotoxicity of MEDI2228 is due to the formation of DNA ICLs after the internalized released warhead binds in the DNA minor groove. MEDI2228 induces multiple DNA damage and repair checkpoint pathways, growth arrest, and apoptosis in MM cells. Furthermore, PBD dimers cause cell death in both rapidly dividing and more quiescent cells, unlike MMAF. Importantly, MM cells harboring p53 mutations, expressing low levels of BCMA, or resistant to current treatments, are all more susceptible to MEDI2228, compared with its MMAF-ADC homolog. These results indicate potential uses of MEDI2228 to deplete tumor cells with heterogeneous BCMA expression and in high-risk MM with intrinsic or acquired drug resistance. For example, MEDI2228 could be highly effective in aggressive tumors inherently resistant to other warhead types, such as MMAF, and in multidrug-resistant MM patients.

MM cells have constitutive DNA damage signaling with diminished DNA damage repair, which underlies their hallmark genome instability [1–3, 50–55]. They are characterized by defects in the systems ensuring strict control of the cell cycle in normal tissues. Their ongoing DNA damage levels compared to surrounding normal cells in the BM microenvironment could provide for a potential therapeutic window for therapeutic agents targeting these processes. Such agents may promote stress replication, impair the ability of MM cells to handle elevated levels of replicative pressure, and impede DNA repair processes. Synergistic lethality between DNA repair pathways and DNA replicative pressure was further shown here by combined treatment with MEDI2228 and 3 major DDRi s. ATMi (AZD0156), ATRi (AZD6738), and WEE1i (AZD1775) each synergize with MEDI2228 even in MM cell lines resistant to btz and IMiDs, as well as in MM cell lines with mutated p53. Blocking stress sensitizers ATM/ATR/WEE1 prevents repair of damaged DNA and induces cell death. Importantly, combining MEDI2228 with these stress sensitization and cell cycle regulatory drugs such as ATMi, ATRi, or WEE1i not only further increases the stress load, but also augments MM cell death. Importantly, MEDI2228-induced ATM/ATR-CHK1/2, as well as CDK1/2 activation, is blocked by these DNA repair inhibitors.

Following activation of DDR and cell cycle checkpoints, MEDI2228 significantly induces γH2AX, a common early marker for DNA damage including ICL-induced DSBs. Following MEDI2228-induced DDRs, the DNA repair protein RAD51 is induced in MM cells before apoptosis occurs. Since treatment with btz can reduce certain DSB repair pathways [56], i.e., RAD51 [49], which are exploited by MM cells to develop resistance to chemotherapy such as melphalan [57, 58], we further explored combination use of btz with MEDI2228.

Importantly, combined treatment of MEDI2228 and btz in vitro first induces synergistic death in all MM cells tested. Using immunoblotting and immunostaining coupled with confocal analysis, MEDI2228-induced RAD51 is reduced by btz, providing a molecular mechanism to enhance MM cell toxicity following combination therapy. Significantly, accumulation of irreversible DNA damage was evidenced by enhanced γH2AX-expressing nuclear micro-foci in MM cells co-incubated with MEDI2228 and btz when compared with either agent alone. Notably, MEDI2228 still synergizes with btz even in btz-resistant ANBL6-BR MM cells in the presence of IL-6, indicating other undefined mechanisms also responsible for synergistic cytotoxicity.

In mice bearing MM1S tumors, M2 showed better in vivo MM cell cytotoxicity than btz as single agent therapy, comparing only one single treatment of M2 vs 6 injections of btz in total at the same sub-optimal dose for each drug. Importantly, inhibition of in vivo tumor burden is further enhanced when MEDI2228 with a single sub-optimal dose is combined with btz. Significant tumor necrosis is observed earlier in mice receiving both drugs than either agent alone; and at 177d, 15% mice in the combination-treatment group remain alive and without tumor. No weight loss is noted in all groups, suggesting a favorable safety profile of MEDI2228 in vivo. Moreover, activation of DDR signaling cascades by M2 potentiates the cytotoxic effects of btz in this human MM xenograft model. The synergistic in vitro and in vivo cytotoxicity strongly supports the potential clinical utility of enhancing DNA damage while inhibiting DNA repair to overcome proteasome inhibitor resistance in MM.

MEDI2228 treatment induces DNA damage and DDR signaling cascades in human MM cells in vivo, associated with key molecular markers for growth arrest and apoptosis. Compared with vehicle control or btz treatment, MEDI2228 significantly upregulates γH2AX-expressing foci in the nuclei, confirming MEDI2228-induced DNA DSBs in vivo. These results indicate that γH2AX is a highly sensitive DDR marker to PBD dimers in vitro and in vivo, in accord with recent studies of similar PBD-ADCs targeting different antigens [37, 59]. Importantly, a marked increase in γH2AX nuclear foci is observed in MM1S tumors excised from mice treated with MEDI2228 and btz vs either agent alone, indicating enhanced accumulation of unrepaired DNA lesions in vivo leading to superior tumor cell death. Thus, the combination of MEDI2228 with btz further augments MM cell killing in vitro and in vivo via synergistic DNA damage-induced lethality.

In summary, MEDI2228 specifically triggers potent growth inhibition and death, even in MM cells resistant to current MM therapies and protected by the BM microenvironment. Unlike its MMAF-ADC homolog, it potently induces ATM/ATR-CHK1/2-CDK1/2 signaling cascades, DNA damage and repair responses, prior to apoptosis of MM cells. Significantly, ATM/ATR/WEE1 inhibitors targeting various phases of cell cycle checkpoints improve sensitivity of MM cells to MEDI2228 via blockade of MEDI2228-induced DDR signaling pathways, thereby achieving DNA damage-induced synergistic MM cell lethality. Moreover, the combination of this BCMA PBD-ADC with btz in vivo significantly enhances efficacy to eradicate tumors over either single agent alone via augmented DNA damages while reducing DNA repair, and further extends host survival. Thus, MEDI2228 can be leveraged with DDRi s or PIs to overcome intrinsic or acquired drug resistance in MM.

Moreover, this study supports ongoing clinical development of MEDI2228 as an ADC monotherapy or in combination with DDRi s or PIs to further prolong remission in RRMM.

Supplementary Material

Refer to Web version on PubMed Central for supplementary material.

Acknowledgements

The authors thank the flow cytometry assistance from the flow cytometry facility at Dana-Farber Cancer Institute. We thank all lab members and the clinical research coordinators of the Jerome Lipper Multiple Myeloma Center and the LeBow Institute for Myeloma Therapeutics of the Dana-Farber Cancer Institute for support and help in providing primary tumor specimens for this study. We would also like to acknowledge Ryan Fleming of AstraZeneca for the preparation and characterization of ADCs used in this study.

Financial support

This work was supported in part by grants from the National Institutes of Health Specialized Programs of Research Excellence (SPORE) P50 CA100707, P01CA155258, and RO1 CA 207237. This work was supported in part by Dr Miriam and Sheldon G Adelson Medical Research Foundation. Dr. Kenneth C. Anderson is an American Cancer Society Clinical Research Professor. This study was funded by AstraZeneca.

References

1. Walters DK, Wu X, Tschumper RC, Arendt BK, Huddleston PM, Henderson KJ, et al. Evidence for ongoing DNA damage in multiple myeloma cells as revealed by constitutive phosphorylation of H2AX. Leukemia. 2011;25:1344–53. [PubMed: 21566653]
2. Cottini F, Hideshima T, Xu C, Sattler M, Dori M, Agnelli L, et al. Rescue of Hippo coactivator YAP1 triggers DNA damage-induced apoptosis in hematological cancers. Nat Med 2014;20:599–606. [PubMed: 24813251]
3. Cottini F, Hideshima T, Suzuki R, Tai YT, Bianchini G, Richardson PG, et al. Synthetic lethal approaches exploiting DNA damage in aggressive myeloma. Cancer discovery. 2015;5:972–87. [PubMed: 26080835]
4. van Nieuwenhuijzen N, Spaan I, Raymakers R, Peperzak V. From MGUS to multiple myeloma, a paradigm for clonal evolution of premalignant cells. Cancer Res 2018;78:2449–56. [PubMed: 29703720]
5. Corre J, Cleynen A, Robiou du Pont S, Buisson L, Bolli N, Attal M, et al. Multiple myeloma clonal evolution in homogeneously treated patients. Leukemia. 2018;32:2636–47. [PubMed: 29895955]
6. Szalat R, Avet-Loiseau H, Munshi NC. Gene expression profiles in myeloma: ready for the real world? Clin Cancer Res 2016;22:5434–42. [PubMed: 28151711]
7. Bolli N, Avet-Loiseau H, Wedge DC, Van Loo P, Alexandrov LB, Martincorena I, et al. Heterogeneity of genomic evolution and mutational profiles in multiple myeloma. Nature communications. 2014;5:2997.
8. Walker BA, Wardell CP, Melchor L, Brioli A, Johnson DC, Kaiser MF, et al. Intraclonal heterogeneity is a critical early event in the development of myeloma and precedes the development of clinical symptoms. Leukemia. 2014;28:384–90. [PubMed: 23817176]
9. Kumar SK, Rajkumar V, Kyle RA, van Duin M, Sonneveld P, Mateos MV, et al. Multiple myeloma. Nat Rev Dis Primers. 2017;3:17046. [PubMed: 28726797]
10. Avet-Loiseau H Introduction to the review series on advances in multiple myeloma. Blood. 2018.
11. Anderson KC. Promise of Immune Therapies in Multiple Myeloma. J Oncol Pract 2018;14:411–3. [PubMed: 29996072]
12. Tai YT, Dillon M, Song W, Leiba M, Li XF, Burger P, et al. Anti-CS1 humanized monoclonal antibody HuLuc63 inhibits myeloma cell adhesion and induces antibody-dependent cellular cytotoxicity in the bone marrow milieu. Blood. 2008;112:1329–37. [PubMed: 17906076]

13. de Weers M, Tai YT, van der Veer MS, Bakker JM, Vink T, Jacobs DC, et al. Daratumumab, a novel therapeutic human CD38 monoclonal antibody, induces killing of multiple myeloma and other hematological tumors. J Immunol 2011;186:1840–8. [PubMed: 21187443]
14. Lokhorst HM, Plesner T, Laubach JP, Nahi H, Gimsing P, Hansson M, et al. Targeting CD38 with daratumumab monotherapy in multiple myeloma. N Engl J Med 2015;373:1207–19. [PubMed: 26308596]
15. Lonial S, Dimopoulos M, Palumbo A, White D, Grosicki S, Spicka I, et al. Elotuzumab therapy for relapsed or refractory multiple myeloma. N Engl J Med 2015;373:621–31. [PubMed: 26035255]
16. Richardson PG, Jagannath S, Moreau P, Jakubowiak AJ, Raab MS, Facon T, et al. Elotuzumab in combination with lenalidomide and dexamethasone in patients with relapsed multiple myeloma: final phase 2 results from the randomised, open-label, phase 1b-2 dose-escalation study. Lancet Haematol 2015;2:e516–27. [PubMed: 26686406]
17. Lonial S, Kaufman J, Reece D, Mateos MV, Laubach J, Richardson P. Update on elotuzumab, a novel anti-SLAMF7 monoclonal antibody for the treatment of multiple myeloma. Expert Opin Biol Ther 2016;16:1291–301. [PubMed: 27533882]
18. Offidani M, Corvatta L. A review discussing elotuzumab and its use in the second-line plus treatment of multiple myeloma. Future Oncol 2018;14:319–29. [PubMed: 29091475]
19. van de Donk N, Richardson PG, Malavasi F. CD38 antibodies in multiple myeloma: back to the future. Blood. 2018;131:13–29. [PubMed: 29118010]
20. Tzogani K, Penninga E, Schougaard Christiansen ML, Hovgaard D, Sarac SB, Camarero Jimenez J, et al. EMA review of daratumumab for the treatment of adult patients with multiple myeloma. Oncologist. 2018;23:594–602. [PubMed: 29371479]
21. Coats S, Williams M, Kebble B, Dixit R, Tseng L, Yao NS, et al. Antibody-drug conjugates: future directions in clinical and translational strategies to improve the therapeutic index. Clin Cancer Res 2019.
22. Tai YT, Mayes PA, Acharya C, Zhong MY, Cea M, Cagnetta A, et al. Novel anti-B-cell maturation antigen antibody-drug conjugate (GSK2857916) selectively induces killing of multiple myeloma. Blood. 2014;123:3128–38. [PubMed: 24569262]
23. Tai YT, Anderson KC. Targeting B-cell maturation antigen in multiple myeloma. Immunotherapy. 2015;7:1187–99. [PubMed: 26370838]
24. Cho SF, Anderson KC, Tai YT. Targeting B cell maturation antigen (BCMA) in multiple myeloma: potential sses of BCMA-based immunotherapy. Front Immunol 2018;9:1821. [PubMed: 30147690]
25. Tai YT, Anderson KC. BCMA-based Immunotherapy for Multiple Myeloma. Expert Opin Biol Ther 2019;in press.
26. Cho SF, Lin L, Xing L, Yu T, Wen K, Anderson KC, et al. Monoclonal Antibody: A New Treatment Strategy against Multiple Myeloma. Antibodies (Basel). 2017;6.
27. Lee L, Bounds D, Paterson J, Herledan G, Sully K, Seestaller-Wehr LM, et al. Evaluation of B cell maturation antigen as a target for antibody drug conjugate mediated cytotoxicity in multiple myeloma. Br J Haematol 2016;174:911–22. [PubMed: 27313079]
28. Trudel S, Lendvai N, Popat R, Voorhees PM, Reeves B, Libby EN, et al. Targeting B-cell maturation antigen with GSK2857916 antibody-drug conjugate in relapsed or refractory multiple myeloma (BMA117159): a dose escalation and expansion phase 1 trial. Lancet Oncol 2018;19:1641–53. [PubMed: 30442502]
29. Trudel S, Lendvai N, Popat R, Voorhees PM, Reeves B, Libby EN, et al. Antibody-drug conjugate, GSK2857916, in relapsed/refractory multiple myeloma: an update on safety and efficacy from dose expansion phase I study. Blood Cancer J 2019;9:37. [PubMed: 30894515]
30. Raje N, Berdeja J, Lin Y, Siegel D, Jagannath S, Madduri D, et al. Anti-BCMA CAR T-cell therapy bb2121 in relapsed or refractory multiple myeloma. N Engl J Med 2019;380:1726–37. [PubMed: 31042825]
31. Cohen AD, Garfall AL, Stadtmauer EA, Melenhorst JJ, Lacey SF, Lancaster E, et al. B cell maturation antigen-specific CAR T cells are clinically active in multiple myeloma. J Clin Invest 2019;130.

32. Brudno JN, Maric I, Hartman SD, Rose JJ, Wang M, Lam N, et al. T cells genetically modified to express an anti-B-cell maturation antigen chimeric antigen receptor cause remissions of poor-prognosis relapsed multiple myeloma. J Clin Oncol 2018;36:2267–80. [PubMed: 29812997]
33. Hipp S, Tai YT, Blanset D, Deegen P, Wahl J, Thomas O, et al. A novel BCMA/CD3 bispecific T-cell engager for the treatment of multiple myeloma induces selective lysis in vitro and in vivo. Leukemia. 2017;31:1743–51. [PubMed: 28025583]
34. Topp MS, Duell J, Zugmaier G, Attal M, Moreau P, Langer C, et al. Evaluation of AMG 420, an anti-BCMA bispecific T-cell engager (BiTE) immunotherapy, in R/R multiple myeloma (MM) patients: Updated results of a first-in-human (FIH) phase I dose escalation study. J Clin Oncol 2019;37:8007-.
35. Kinneer K, Flynn M, Thomas SB, Meekin J, Varkey R, Xiao X, et al. Preclinical assessment of an antibody-PBD conjugate that targets BCMA on multiple myeloma and myeloma progenitor cells. Leukemia. 2019;33:766–71. [PubMed: 30315237]
36. Rudin CM, Pietanza MC, Bauer TM, Ready N, Morgensztern D, Glisson BS, et al. Rovalpituzumab tesirine, a DLL3-targeted antibody-drug conjugate, in recurrent small-cell lung cancer: a first-in-human, first-in-class, open-label, phase 1 study. Lancet Oncol 2017;18:42–51. [PubMed: 27932068]
37. Zammarchi F, Corbett S, Adams L, Tyrer PC, Kiakos K, Janghra N, et al. ADCT-402, a PBD dimer-containing antibody drug conjugate targeting CD19-expressing malignancies. Blood. 2018;131:1094–105. [PubMed: 29298756]
38. Dimasi N, Fleming R, Zhong H, Bezabeh B, Kinneer K, Christie RJ, et al. Efficient preparation of site-specific antibody-drug conjugates using cysteine insertion. Mol Pharm 2017;14:1501–16. [PubMed: 28245132]
39. Jiang H, Acharya C, An G, Zhong M, Feng X, Wang L, et al. SAR650984 directly induces multiple myeloma cell death via lysosomal-associated and apoptotic pathways, which is further enhanced by pomalidomide. Leukemia. 2016;30:399–408. [PubMed: 26338273]
40. Tai YT, Chang BY, Kong SY, Fulciniti M, Yang G, Calle Y, et al. Bruton tyrosine kinase inhibition is a novel therapeutic strategy targeting tumor in the bone marrow microenvironment in multiple myeloma. Blood. 2012;120:1877–87. [PubMed: 22689860]
41. Tai YT, Landesman Y, Acharya C, Calle Y, Zhong MY, Cea M, et al. CRM1 inhibition induces tumor cell cytotoxicity and impairs osteoclastogenesis in multiple myeloma: molecular mechanisms and therapeutic implications. Leukemia. 2014;28:155–65. [PubMed: 23588715]
42. Tai YT, Acharya C, An G, Moschetta M, Zhong MY, Feng X, et al. APRIL and BCMA promote human multiple myeloma growth and immunosuppression in the bone marrow microenvironment. Blood. 2016;127:3225–36. [PubMed: 27127303]
43. Long DT, Raschle M, Joukov V, Walter JC. Mechanism of RAD51-dependent DNA interstrand cross-link repair. Science. 2011;333:84–7. [PubMed: 21719678]
44. Lin AB, McNeely SC, Beckmann RP. Achieving Precision Death with Cell-Cycle Inhibitors that Target DNA Replication and Repair. Clin Cancer Res 2017;23:3232–40. [PubMed: 28331049]
45. Pike KG, Barlaam B, Cadogan E, Campbell A, Chen Y, Colclough N, et al. The identification of potent, selective, and orally available inhibitors of Ataxia Telangiectasia Mutated (ATM) kinase: the discovery of AZD0156 (8-{6-[3-(Dimethylamino)propoxy]pyridin-3-yl}−3-methyl-1-(tetrahydro-2 H-pyran-4-yl)-1,3-dihydro-2 H-imidazo[4,5- c]quinolin-2-one). J Med Chem 2018;61:3823–41. [PubMed: 29683659]
46. Foote KM, Nissink JWM, McGuire T, Turner P, Guichard S, Yates JWT, et al. Discovery and characterization of AZD6738, a potent inhibitor of Ataxia Telangiectasia Mutated and Rad3 Related (ATR) kinase with application as an anticancer agent. J Med Chem 2018;61:9889–907. [PubMed: 30346772]
47. Fu S, Wang Y, Keyomarsi K, Meric-Bernstam F, Meric-Bernstein F. Strategic development of AZD1775, a Wee1 kinase inhibitor, for cancer therapy. Expert Opin Investig Drugs. 2018;27:741–51.
48. Chou TC. Drug combination studies and their synergy quantification using the Chou-Talalay method. Cancer Res 2010;70:440–6. [PubMed: 20068163]

49. Neri P, Ren L, Gratton K, Stebner E, Johnson J, Klimowicz A, et al. Bortezomib-induced "BRCAness" sensitizes multiple myeloma cells to PARP inhibitors. Blood. 2011;118:6368–79. [PubMed: 21917757]
50. Tai YT, Teoh G, Lin B, Davies FE, Chauhan D, Treon SP, et al. Ku86 variant expression and function in multiple myeloma cells is associated with increased sensitivity to DNA damage. J Immunol 2000;165:6347–55. [PubMed: 11086072]
51. Tai YT, Podar K, Kraeft SK, Wang F, Young G, Lin B, et al. Translocation of Ku86/Ku70 to the multiple myeloma cell membrane: functional implications. Experimental hematology. 2002;30:212–20. [PubMed: 11882358]
52. Dimopoulos MA, Souliotis VL, Anagnostopoulos A, Bamia C, Pouli A, Baltadakis I, et al. Melphalan-induced DNA damage in vitro as a predictor for clinical outcome in multiple myeloma. Haematologica. 2007;92:1505–12. [PubMed: 18024399]
53. Neri P, Bahlis NJ. Genomic instability in multiple myeloma: mechanisms and therapeutic implications. Expert Opin Biol Ther 2013;13 Suppl 1:S69–82. [PubMed: 23782016]
54. Cea M, Cagnetta A, Adamia S, Acharya C, Tai YT, Fulciniti M, et al. Evidence for a role of the histone deacetylase SIRT6 in DNA damage response of multiple myeloma cells. Blood. 2016;127:1138–50. [PubMed: 26675349]
55. Szalat R, Samur MK, Fulciniti M, Lopez M, Nanjappa P, Cleynen A, et al. Nucleotide excision repair is a potential therapeutic target in multiple myeloma. Leukemia. 2018;32:111–9. [PubMed: 28588253]
56. Chen S, Blank JL, Peters T, Liu XJ, Rappoli DM, Pickard MD, et al. Genome-wide siRNA screen for modulators of cell death induced by proteasome inhibitor bortezomib. Cancer Res 2010;70:4318–26. [PubMed: 20460535]
57. Spanswick VJ, Craddock C, Sekhar M, Mahendra P, Shankaranarayana P, Hughes RG, et al. Repair of DNA interstrand crosslinks as a mechanism of clinical resistance to melphalan in multiple myeloma. Blood. 2002;100:224–9. [PubMed: 12070031]
58. Gkotzamanidou M, Terpos E, Bamia C, Munshi NC, Dimopoulos MA, Souliotis VL. DNA repair of myeloma plasma cells correlates with clinical outcome: the effect of the nonhomologous end-joining inhibitor SCR7. Blood. 2016;128:1214–25. [PubMed: 27443291]
59. Flynn MJ, Zammarchi F, Tyrer PC, Akarca AU, Janghra N, Britten CE, et al. ADCT-301, a pyrrolobenzodiazepine (PBD) dimer-containing antibody-drug conjugate (ADC) targeting CD25-expressing hematological malignancies. Molecular cancer therapeutics. 2016;15:2709–21. [PubMed: 27535974]

Key points:

- Multiple DNA damage response (DDR) pathways are activated by a novel BCMA PBD-ADC in MM cells regardless of BCMA levels, p53 status, and drug resistance.
- MEDI2228 synergizes with ATM/ATR/WEE1 inhibitors or bortezomib to further prevent DNA repair to augment MM cell lethality.

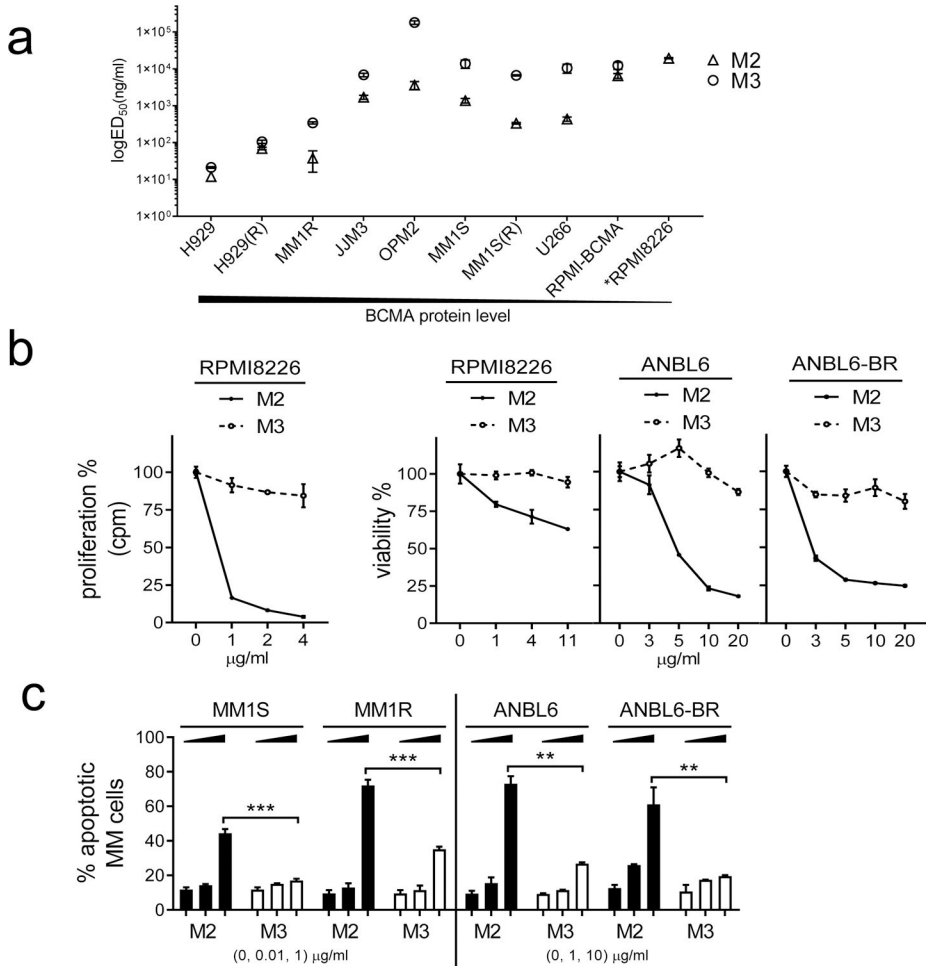

Fig. 1. MEDI2228 (M2) induces more potent cytotoxicity against MM cells than its MMAF-ADC homolog (M3).

a Serial dilution of M2 or M3 were added into MM cell cultures for 3d followed by CCK8 cell viability assay. BCMA protein levels determined by flow cytometry (FCM) analysis (at the bottom) are highest and lowest in H929 and RPMI8226, respectively. Shown are ED_{50} values for M2 (open triangle) and M3 (open circle). Data represent the mean (± standard deviation, SD) of three independent experiments, each performed in triplicate at each dose. Error bars indicate SDs. H929(R) and MM1S(R) cells derived from H929 and MM1S, respectively, are resistant to both len and pom. RPMI-BCMA, RPMI8226 cells overexpressing BCMA; *RPMI8226, relatively insensitive to M3 due to unavailable ED_{50} (see also in **b**). **b** M2 (asterisk, solid line) or M3 (open circle, dash line) were added for 3d, followed by cell proliferation assay using [H^3] thymidine incorporation (left) in RPMI8226 cells. Viability assays (right) are based on CCK8 for RPMI8226 and luminescent-based Cell-Titer Growth (CTG) for paired ANBL6 and ANBL6-BR (bortezomib (btz)-resistant) MM cells. **c** Dexamethasone (dex) (MM1S/MM1R)- and btz (ANBL6/ANBL6-BR)-resistant cell pairs were treated with M2 or M3 for 2d, followed by FCM analysis to determine percentages of apoptotic cells (Annexin V+/Aqua− and Annexin V+/Aqua+). ***, $p<0.0005$; **, $p<0.005$. Each experiment was performed at least thrice in triplicate for each dose, and data are represented as mean ± SD.

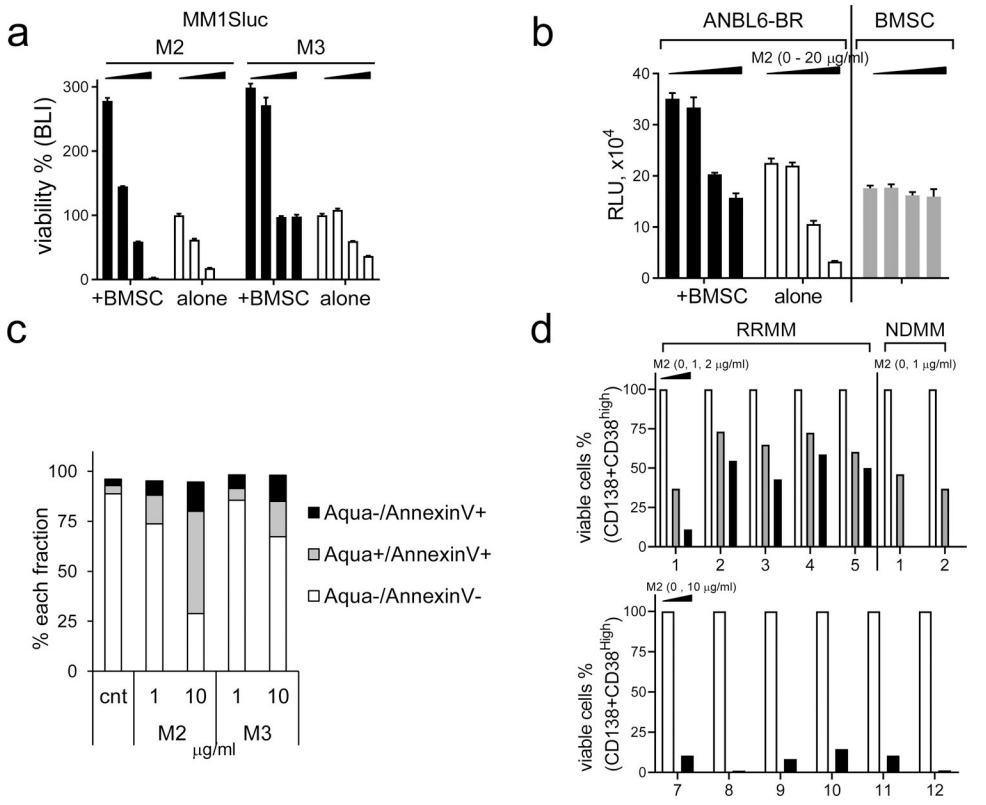

Fig. 2. M2, more potently than M3, inhibits BMSC-induced MM cell viability and MM cells from patients.

a MM1Sluc cells, alone or with BMSCs, were treated with M2 or M3 (0, 0.05, 0.1, 0.2 μg/ml) for 4d, and cell viability was determined by BLI. **b** Btz-resistant ANBL6-BR, with or without BMSCs, were treated with M2 followed by CTG assay. **c** CD138+ cells from a representative RRMM patient were incubated with M2 or M3 for 3d, and live/dead cell fractions were measured by quantitative flow cytometry analysis. **d** BM mononuclear cells of RRMM and NDMM patients were treated with M2 for 1d (upper panel) or 3d (RRMM 7–12, lower panel). Patient MM cells were protected by their surrounding non-MM cells to test effects of M2. Percentages of viable CD38highCD138+ cells were determined by FCM analysis.

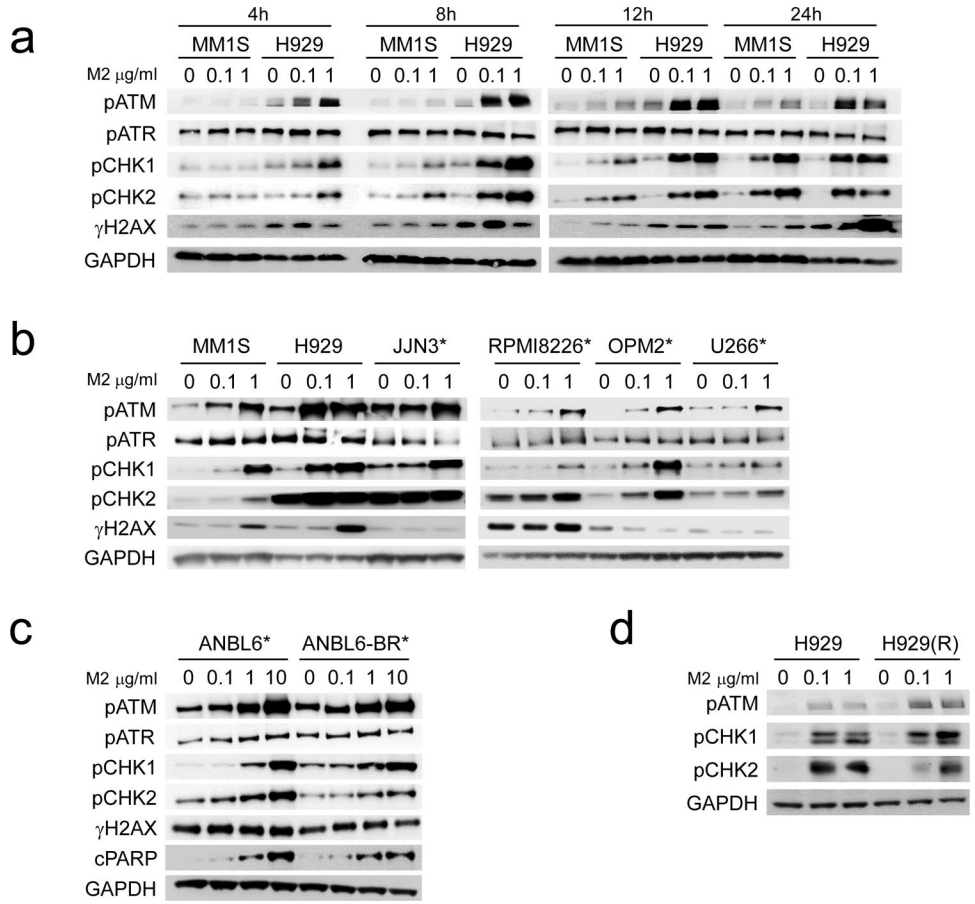

Fig. 3. M2 significantly induces phosphorylation of DNA damage response (DDR) signaling pathways in MM cells, regardless of p53 status and drug resistance.

MM cells with wild type (MM1S, MM1R, H929) and mutated p53 (*) were treated with indicated doses of M2 (**a-d**) for indicated time periods (**a**), overnight (**b**, **d**), or 2d (**c**). Cell lysates were prepared and analyzed by immunoblotting using specific antibodies for indicated molecules. cPARP, cleaved PARP; cCas3, cleaved caspase 3. Experiments were repeated three times.

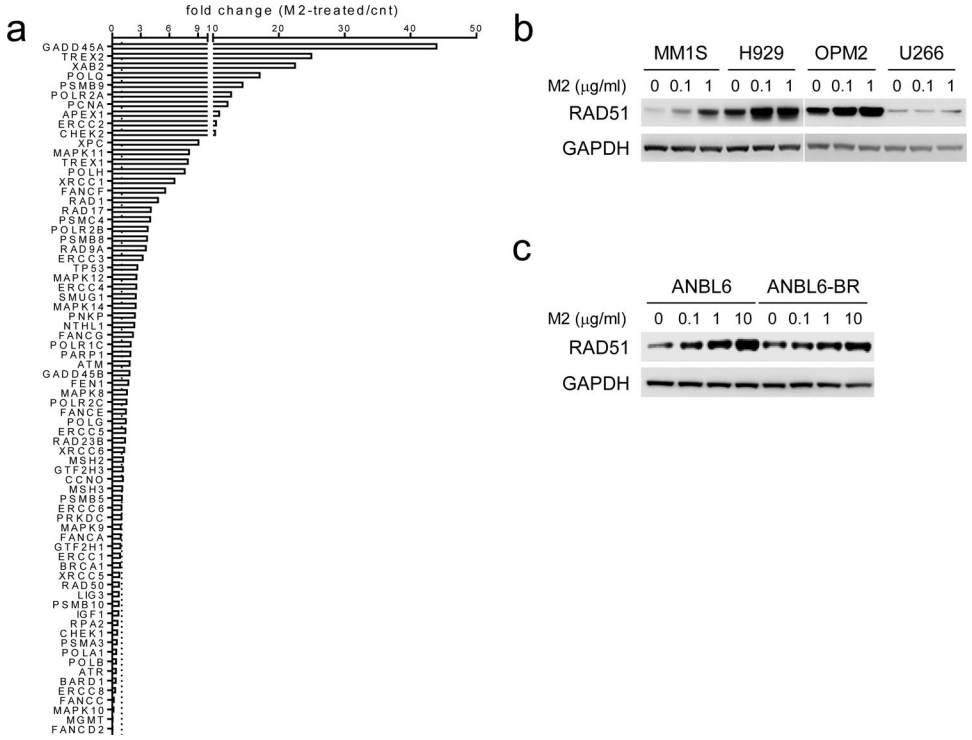

Fig. 4. M2 treatment induces DDR-related gene expression including RAD51.

a RNA from viable H929 MM cells treated with M2 under sub-lethal conditions were analyzed using the TaqMan® human DNA Repair pathway array. Transcripts were normalized by geomean of internal controls, and fold changes in M2-treated relative to control (cnt) groups are shown. **b-c** Cell lysates were made from various M2-treated MM cell lines for immunoblotting to determine protein levels of RAD51.

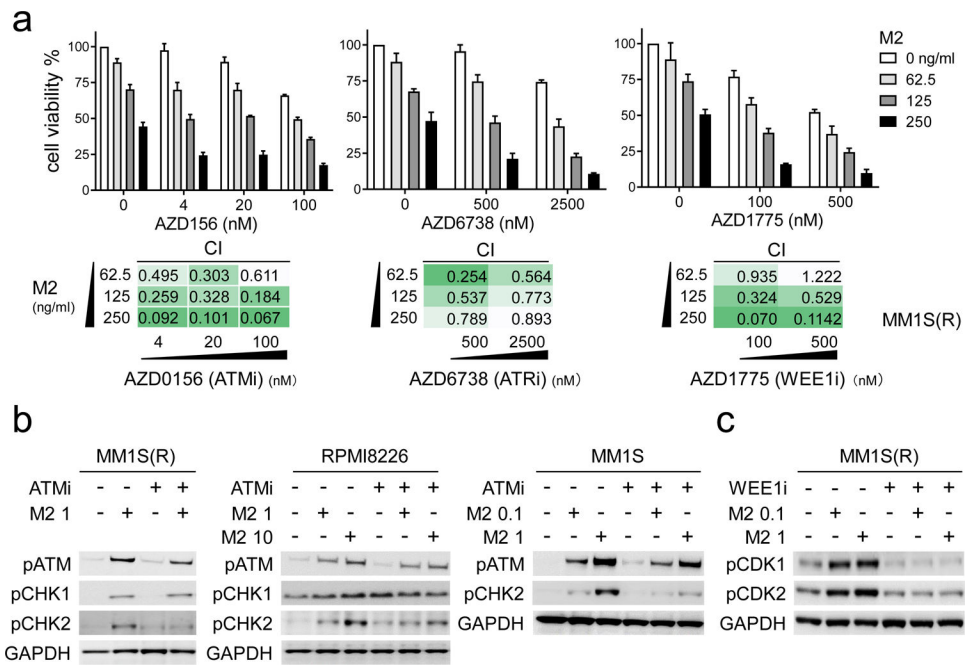

Fig. 5. Combined treatments with M2 and DDR inhibitors (DDRi s) cause synthetic lethality in drug-sensitive and -resistant MM cells.

a IMiD-resistant MM1S(R) cells were co-treated for 3d with M2, as indicated on the legend (upper panel) and the rows (lower panel), and various concentrations of the indicated DDR inhibitor (DDRi), as indicated on the x-axis (upper panel) and the columns (lower panel), either alone or in combination. Shown are means ± SDs of 3 independent experiments with each performed in triplicate at each dose. Error bars indicate SDs. Values of combination index (CI), determined by CTG-based assays, are shown below each graph in various levels in green. CI < 1 indicates synergism of both drugs. **b-c** Indicated MM cells treated with M2 (μg/mL) in the presence (+) or absence (−) of ATMi (AZD0156, 0.1 μM) (**b**) or WEE1i (AZD1775, 0.5 μM) (**c**), alone or together, were subjected to lysate preparation for immunoblotting analysis for indicated molecules.

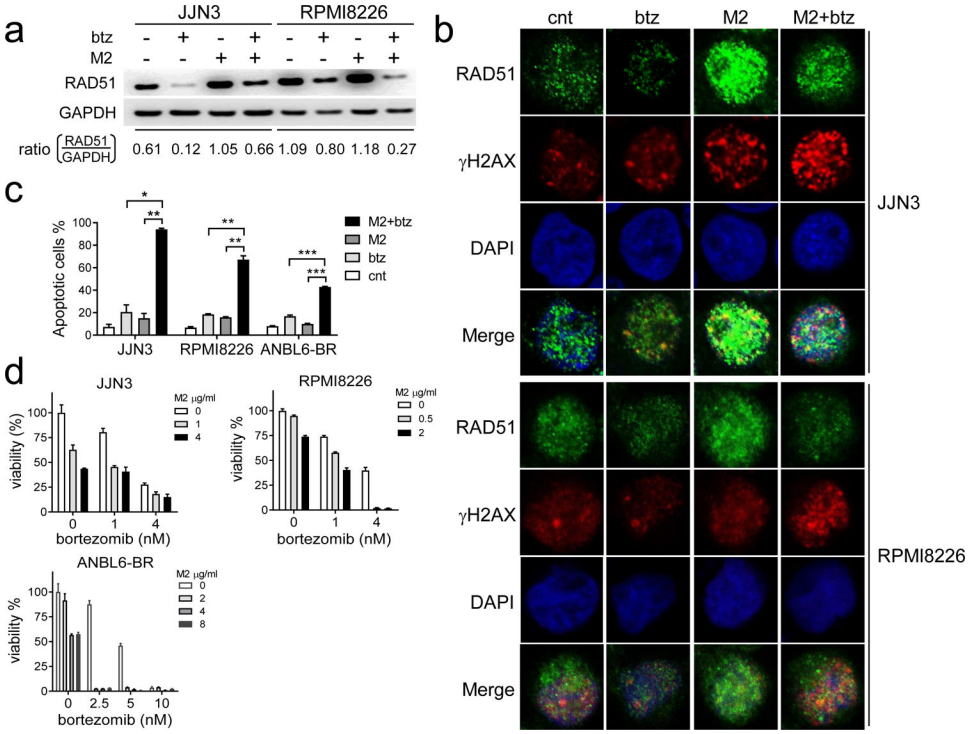

Fig. 6. M2 co-treated with bortezomib synergistically induces MM cell death.

a-b Indicated MM cells treated with of M2 (4μg/ml) or bortezomib (btz) (4 nM) under sublethal conditions, alone or together, were subject to (**a**) lysate preparation for immunoblotting analysis or (**b**) immunofluorescence analysis to assay RAD51 and γH2AX levels. **b** Immunofluorescence assay followed by confocal microscopy analysis was conducted to monitor foci formation of RAD51 (green) and γH2AX (red) to determine DNA damage accumulation coupled with a decreased repair capacity in cells treated with both drugs. **c** MM cells were treated with M2 (4μM) and btz (4nM) for 2d, followed by FCM analysis using PI and Annexin V staining. Shown are means % of Annexin V+ cells ± SDs of 3 independent experiments with triplicates at each treatment condition. *, $p<0.01$; **, $p<0.005$, ***, $p<0.002$. **d** Shown are means ± SDs of the means of 3 independent experiments. CI < 1 indicates synergism of both drugs (Supplemental Fig. S5B).

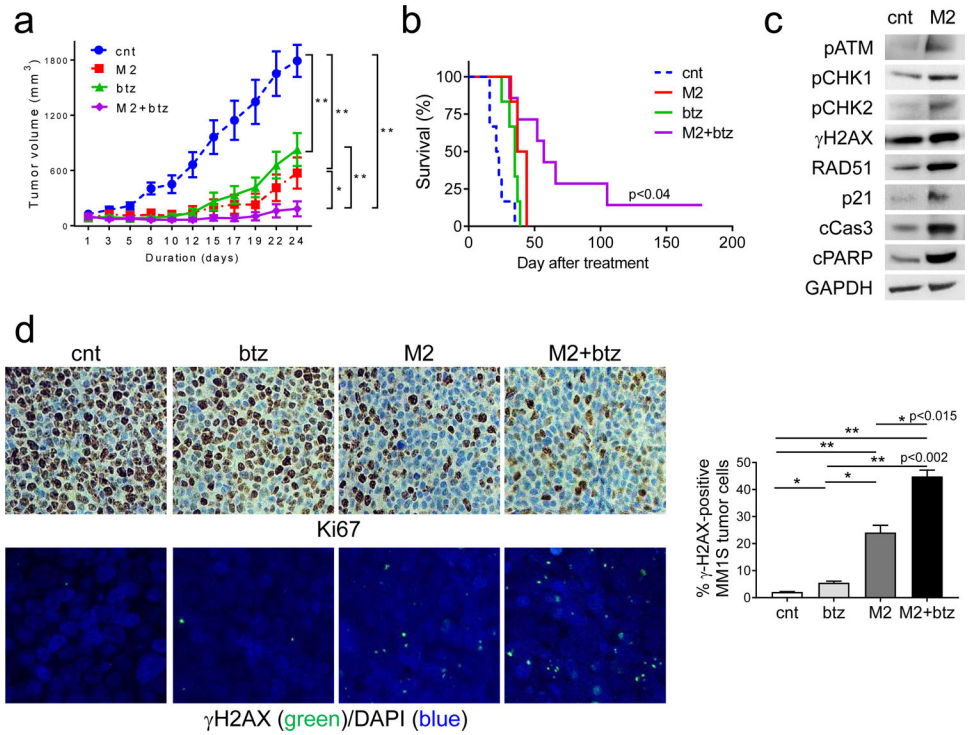

Fig. 7. M2 combined with bortezomib induces more potent in vivo anti-MM activity and prolonged survival in mice, when compared with individual drug alone.

a CB17 SCID mice (n=7 each group) with palpable MM1S tumor implants were randomized and treated with control vehicle (cnt), a single dose of M2 (0.4 mg/kg), six doses of btz (0.4 mg/kg each dose), or combination of M2 and btz (M2+btz) for 2 weeks. Tumor growth was significantly inhibited in the combination-treated group compared with controls (cnt). (M2 vs M2+btz, p=0.035; btz vs M2+btz, p<0.005; cnt vs M2+btz; p=0.0012; btz vs cnt, p<0.005; M2 vs cnt, p<0.005). *, p<0.04, **, p<0.005. **b** Using Kaplan-Meier and log-rank analysis, the median overall survival of animals treated with combination therapy was significantly prolonged. (cnt, 22d; M2, 40.5d; btz, 35d; M2+btz, 57d) (M2 vs M2+btz, p<0.04; btz vs M2+btz, p<0.023; cnt vs M2+btz, p<0.002). **c** Tumors were removed from mice after 3d treatment with M2 and cnt, followed by immunoblotting analysis using indicated antibodies. **d** Tumor tissue sections from each group were immunohistochemically analyzed for Ki-67 (upper panel, original magnification, x400). Confocal microscopy (lower panel) was performed to visualize γH2AX-expressing micronuclei formation following immunofluorescence-staining with γH2AX (green) and counterstaining with DAPI (blue). Confocal microscopy detecting nuclear γH2AX-positivity (green) scored for each group is summarized on the right. *, $p < 0.05$; **, $p < 0.01$